



## FAR-IR SPECTRAL CHANGES ACCOMPANYING PROTON IRRADIATION OF SOLIDS OF ASTROCHEMICAL INTEREST

REGGIE L. HUDSON<sup>1</sup> and MARLA H. MOORE<sup>2</sup>

<sup>1</sup>Department of Chemistry, Eckerd College, St Petersburg, FL 33733 and <sup>2</sup>Astrochemistry Branch, NASA/Goddard Space Flight Center, Greenbelt, MD 20771, U.S.A.

(Received 6 August 1993; accepted 22 June 1994)

**Abstract**—Far-infrared spectroscopy was used to investigate crystalline-to-amorphous phase changes in irradiated solids. Radiation-induced changes at  $T \leq 77$  K were studied in four solids of astrochemical interest:  $\text{H}_2\text{O}$ ,  $\text{CH}_3\text{OH}$ ,  $\text{H}_2\text{CO}$ , and  $\text{CO}_2$ . Rates of amorphization were compared for  $\text{H}_2\text{O}$  and  $\text{CH}_3\text{OH}$ . The behavior of each irradiated sample was observed on subsequent warming. Applications of the data to astronomical problems are given.

### INTRODUCTION

Small molecules, such as  $\text{H}_2\text{O}$  and  $\text{CH}_3\text{OH}$ , are central to astrochemical studies of objects such as interstellar ices, the nuclei of comets, planetary rings, and satellites of the outer planets. In each case the object of interest is exposed to cosmic radiation and suffers radiation damage. Such changes can be investigated in the laboratory by irradiation of molecular solids at low temperature and measurement of some property, such as a spectrum. Of particular interest to astronomers are questions such as (i) how the spectra of various molecules change as they are irradiated, (ii) what phase changes take place during irradiation, (iii) how the properties of the molecules are altered with increasing radiation dose, and (iv) the specific products of solid-phase irradiation and their fates. In this paper we report experiments related primarily to the first two points, how the far-IR spectra of polycrystalline solids respond to ionizing radiation and how crystalline phases of four different materials are altered by irradiation.

Our work has many applications because while various astronomical objects have been exposed to ionizing radiation, the theoretical models used to describe such objects commonly employ data from experiments on *unirradiated* materials. The experiments we describe contribute to an understanding of the behavior of irradiated materials and hence of astronomical objects. Furthermore, we believe that publication of our work is timely. The ESA/ISO space-based telescope to be launched in 1995 will have the ability to record high-quality far-IR spectra of astronomical objects. Interpretation of such spectra will require consideration of laboratory data, such as we report here.

The study of phase changes produced by ionizing radiation has a long history. In 1901, Becquerel reported that ionizing radiation altered the crystal structure of white phosphorus (Becquerel, 1901). Since the 1940's an enormous amount of work has been done on the irradiation of polymers, with much attention being given to changes in crystallinity (Zhang *et al.*, 1992; Charlesby, 1987; Ahmad *et al.*, 1980; Slichter and Mandel, 1958). Perhaps less known are other radiation studies investigating crystalline-to-amorphous phase changes in quartz (Berman *et al.*, 1950), lunar dust grains (Bibring *et al.*, 1972) and, most recently,  $\text{C}_{60}$  molecules (Musket *et al.*, 1991).

Given this history of the irradiation of crystalline solids, it might be thought that crystalline-to-amorphous changes would have been thoroughly investigated in any molecule of interest to astrochemists. The opposite is in fact the case, perhaps due to the difficulty of preparing, stabilizing, and identifying amorphous phases of small molecules. An important aspect of the present paper is that we have assembled an experimental apparatus in which amorphous and crystalline solids can be prepared and identified and the influence of ionizing radiation on them examined *in situ*. It is especially important to appreciate this last point, that all of our work is being done on solids, since in many previous studies on irradiated ices, the solids have been melted immediately after the irradiation. While those experiments have been invaluable for investigating product yields and reaction mechanisms, they are of a very different nature and focus from those to be described here. In addition, most of the earlier experiments used irradiation temperatures at or above 77 K, and radiation of low stopping power, such as electrons, X-rays, or  $^{60}\text{Co}$   $\gamma$  rays. Experiments at lower tempera-

tures with radiation of higher stopping powers are much more relevant for astrochemical work.

Our choice of molecules is particularly significant in that we have selected small molecules of interest to astrochemists, namely water ( $\text{H}_2\text{O}$ ), methanol ( $\text{CH}_3\text{OH}$ ), formaldehyde ( $\text{H}_2\text{CO}$ ), and carbon dioxide ( $\text{CO}_2$ ). Finally, infrared (IR) spectroscopy, a technique amenable to astronomical usage, was selected to study radiation damage.

#### EXPERIMENTAL

Many of the experimental details concerning our work have been published (Moore and Hudson, 1992, 1994; Hudson and Moore, 1992). However, some description of our procedures and choice of conditions may be useful.

Figure 1 is a schematic of the experimental arrangement. Briefly, solid samples were prepared by slow condensation from the vapor phase (gas-handling system) at  $T \sim 295$  K onto the polished face (area =  $5 \text{ cm}^2$ ) of an aluminum substrate held at 13 K in a vacuum chamber. A Fourier-transform IR (FTIR) spectrometer then recorded the spectrum of the solid in the region of interest, usually  $100\text{--}500 \text{ cm}^{-1}$  in these experiments. Next, the sample was rotated  $180^\circ$  to face the beam of our Van de Graaff accelerator, irradiated to the desired dose, and then rotated back to face the spectrometer where its spectrum was recorded a second time. Additional irradiations could be performed as desired with IR spectra taken after each. Single-beam IR spectra were ratioed against the spectrum of the blank aluminum substrate to get a transmission-type spectrum which

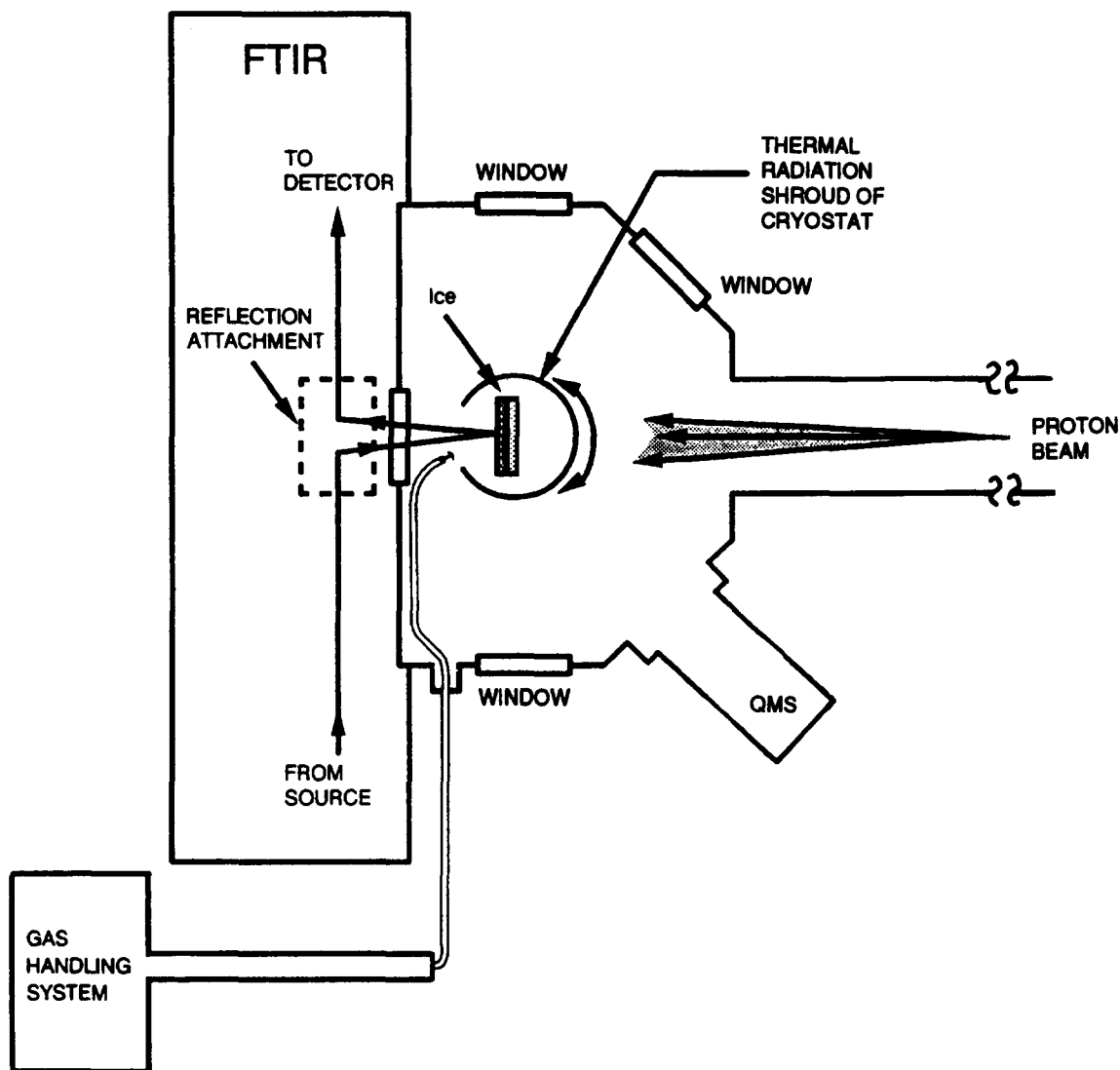


Fig. 1. Experimental set-up showing FTIR spectrometer, incoming radiation beam, gas handling system, and ice sample (on aluminum substrate and facing FTIR). QMS = quadrupole mass spectrometer.

could be converted into an absorbance spectrum. The spectral resolution was  $4\text{ cm}^{-1}$ .

A closed-cycle cryostat was used to cool the samples to a minimum of 13 K. The sample temperature was adjustable before, during, and after the irradiation from 13 to about 280 K with an accuracy better than  $\pm 1\text{ K}$ . Each of the four compounds studied was irradiated at 13 K and two were studied at higher temperatures as well.

The choice of far-IR spectroscopy to study radiation effects deserves comment. Molecular spectra in the mid-IR region,  $\sim 400\text{--}4000\text{ cm}^{-1}$ , correspond to intramolecular vibrational changes. In contrast, far-IR spectra of solids are more sensitive to intermolecular changes, such as translational motions. These low-frequency vibrations are sufficiently dependent upon the phase of the sample that far-IR spectra of the crystalline and amorphous forms of a solid can be quite different from each other. In the experiments to be described, far-IR spectroscopy was used to probe radiation-induced changes in polycrystalline ice samples.

Sample thicknesses were on the order of a few micrometers. They were determined for  $\text{H}_2\text{O}$ ,  $\text{CH}_3\text{OH}$ , and  $\text{CO}_2$  using optical constants (Hudgins *et al.*, 1993; Warren, 1986). Optical constants were unavailable for  $\text{H}_2\text{CO}$  so that the  $\text{H}_2\text{CO}$  sample's thickness could only be estimated from the pressure drop in the vacuum system during deposition. With the thicknesses used, the incident 0.7 MeV protons, having a range of  $\sim 13\text{ }\mu\text{m}$  (Northcliffe and Shilling, 1970), penetrated each solid and came to rest in the underlying aluminum substrate where the resulting current was measured.

In our experiments the effects of cosmic ray bombardment were investigated with 0.7 MeV protons. This choice of radiation was a compromise. Protons form the bulk of cosmic radiation particles and of these the largest flux is for those with energies under 100 MeV (Meyer *et al.*, 1974). Furthermore, standard tables show that the maximum stopping power for protons by  $\text{H}_2\text{O}$  corresponds to an energy near 1 MeV (Northcliffe and Shilling, 1970). This implies that a substantial fraction of the radiation damage to astronomical objects is expected to be due to  $\sim 1\text{ MeV}$  protons. Additional factors concerning our choice of energy were that too high an energy might have induced nuclear transformations in the sample while too low an energy would have meant that the protons would not have completely penetrated the samples. Additional details can be found in earlier papers (Moore *et al.*, 1983; Moore, 1984).

Irradiations were performed with a Van de Graaff accelerator interfaced to our sample chamber. A nickel foil, used to separate the sample and accelerator vacuum systems, degraded the 1 MeV proton energy from the accelerator to 0.7 MeV. A beam current of  $0.1\text{ }\mu\text{A}$  was used to give incident fluences of  $1 \times 10^{13}\text{ p}^+\text{ cm}^{-2}$  to  $1 \times 10^{14}\text{ p}^+\text{ cm}^{-2}$ , although higher doses were employed in a few experiments.

Converting the incident proton fluence into an absorbed energy dose with units of Mrad, MGy, or eV molecule $^{-1}$  required a value for the sample's stopping power which in turn required the sample's density. Since the densities largely were unknown they were assumed to be  $1\text{ g cm}^{-3}$ . Justification for this value comes from structural studies in other laboratories (Narten *et al.*, 1976; Tauer and Lipscomb, 1952). The stopping power ( $S$ ) of 0.7 MeV protons by  $\text{H}_2\text{O}$  is  $430\text{ MeV cm}^2\text{ g}^{-1}$  (Northcliffe and Shilling, 1970). Standard stopping power theory (Magee and Chatterjee, 1987) and mean excitations energies (Fano, 1963) were used to compute  $S = 450\text{ MeV cm}^2\text{ g}^{-1}$  for  $\text{CH}_3\text{OH}$ . The conversions employed in our work with  $\text{H}_2\text{O}$  were  $1 \times 10^{13}\text{ p}^+\text{ cm}^{-2} = 68.6\text{ Mrad} = 0.686\text{ MGy} = 0.128\text{ eV molecule}^{-1}$ , and with  $\text{CH}_3\text{OH}$  they were  $1 \times 10^{13}\text{ p}^+\text{ cm}^{-2} = 72.0\text{ Mrad} = 0.720\text{ MGy} = 0.239\text{ eV molecule}^{-1}$ .

## RESULTS

With each system examined, slow condensation of the sample gas onto the 13 K substrate produced an amorphous solid. Amorphous  $\text{H}_2\text{O}$ ,  $\text{CH}_3\text{OH}$ ,  $\text{H}_2\text{CO}$ , and  $\text{CO}_2$  then could be crystallized by warming to 155, 130, 85, and 65 K, respectively, and holding at the higher temperature for about 5 min before recooling to the irradiation temperature. The preparation of amorphous and crystalline forms of these compounds by vapor deposition has been studied and far-IR spectra published (e.g. Moore and Hudson, 1994 and references therein). Water, in particular, has been subjected to a wide variety of spectroscopic, diffraction, and calorimetric experiments in the past (Hobbs, 1974). Solid  $\text{CO}$  and  $\text{CH}_4$  initially were considered for irradiation but these two molecules lacked suitable far-IR absorbances.

Figure 2 shows far-IR spectra of amorphous and crystalline  $\text{H}_2\text{O}$  at 13 K. The amorphous phase's spectrum, shown in Fig. 2(a) was converted to the crystalline's phase's spectrum, shown in Fig. 2(b) by warming the amorphous sample from 13 to 155 K and then recooling to 13 K. Irradiation of the crystalline sample at 13 K converted its far-IR spectrum into one that was a combination of the spectra of the amorphous and crystalline solids. An example is shown as Fig. 2(c), the incident radiation fluence in the case shown being  $8 \times 10^{13}\text{ p}^+\text{ cm}^{-2}$ . By assuming that only the amorphous and the cubic  $I_c$  phases of solid  $\text{H}_2\text{O}$  contributed to the large absorption peak at  $230\text{ cm}^{-1}$  it was possible to quantify the rate of radiation-induced amorphization. The calculated quantity was designated  $f_c$ , the fraction of crystalline ice remaining after some radiation dose. The Appendix gives additional details of the calculation.

The semi-logarithmic plot in Fig. 3 demonstrates that the amorphization of polycrystalline  $\text{H}_2\text{O}$  was exponential with dose and follows the simple equation  $f_c = e^{-kD}$  where  $k$  is a constant and  $D$  is

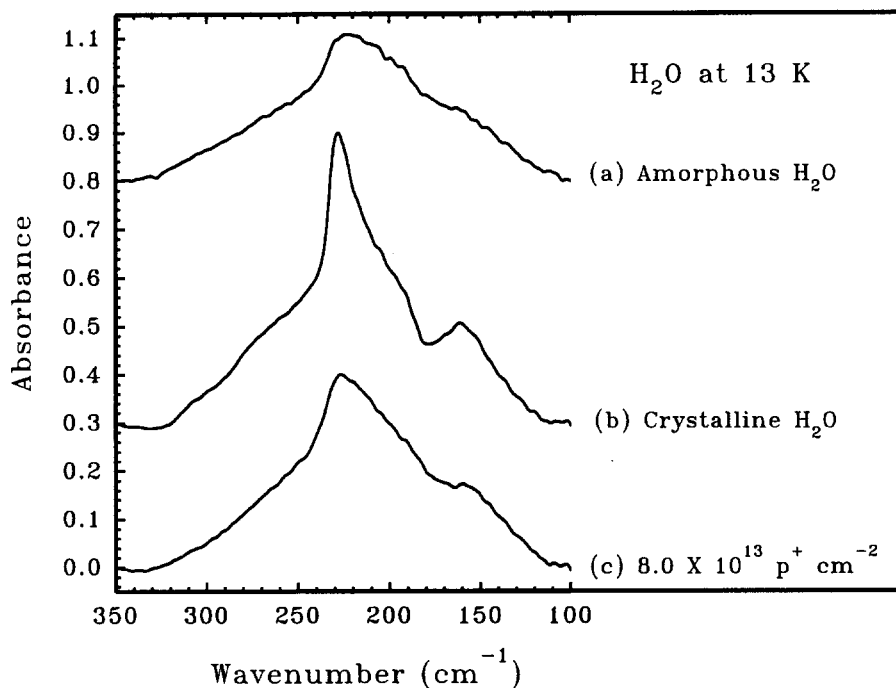


Fig. 2. Far-IR spectra of amorphous, crystalline, and irradiated  $\text{H}_2\text{O}$  at 13 K. Spectra have been offset vertically for clarity. The crystalline sample in (b) was obtained by warming the sample from (a) to 155 K and recooling to 13 K.

dose. The experiment was repeated at 77 K and at that temperature virtually no changes were seen up to a dose of  $1.6 \times 10^{15} \text{ p}^+ \text{ cm}^{-2}$ . This 77 K result is represented by the dashed horizontal line across the top of Fig. 3.

The constant  $k$  for each of six irradiation temperatures was obtained from the slopes of the appropriate lines, such as those in Fig. 3, and is plotted for  $\text{H}_2\text{O}$

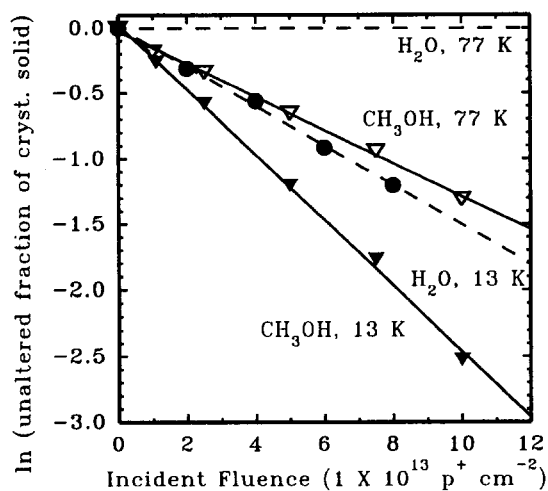


Fig. 3. Radiation-induced amorphization of  $\text{H}_2\text{O}$  and  $\text{CH}_3\text{OH}$  at 13 and 77 K. Conversion of the incident fluences to doses in Mrad requires multiplication by  $(68.6 \text{ Mrad}/1 \times 10^{13} \text{ p}^+ \text{ cm}^{-2})$  for  $\text{H}_2\text{O}$  and  $(72.0/1 \times 10^{13} \text{ p}^+ \text{ cm}^{-2})$  for  $\text{CH}_3\text{OH}$ .

in Fig. 4 against temperature. The appropriate conversion in going from Fig. 3's slope to Fig. 4's vertical scale is  $1.0 \text{ eV molecule}^{-1} = 7.8 \times 10^{13} \text{ p}^+ \text{ cm}^{-2}$ . The constant  $k$ , with units of  $\text{molecule eV}^{-1}$  in Fig. 4, can be interpreted as the number of phase-converted  $\text{H}_2\text{O}$  molecules for a  $1 \text{ eV molecule}^{-1}$  radiation dose. A qualitative interpretation of the temperature dependence of  $k$  will be given below.

An unexpected and unreported oscillatory behavior was discovered in the 13 K irradiation

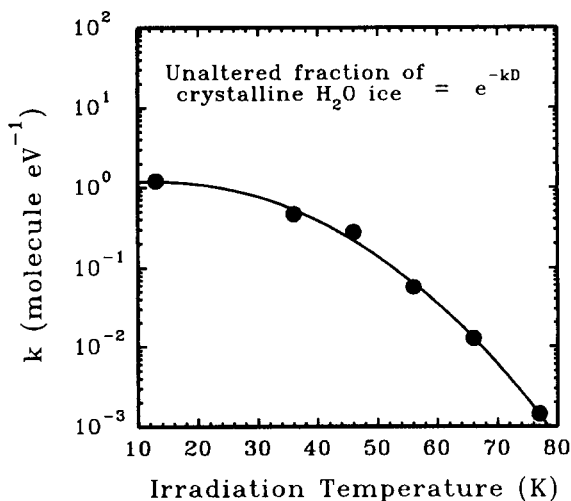


Fig. 4. Temperature dependence of the decay constant " $k$ " for the radiation-induced amorphization of crystalline  $\text{H}_2\text{O}$ .

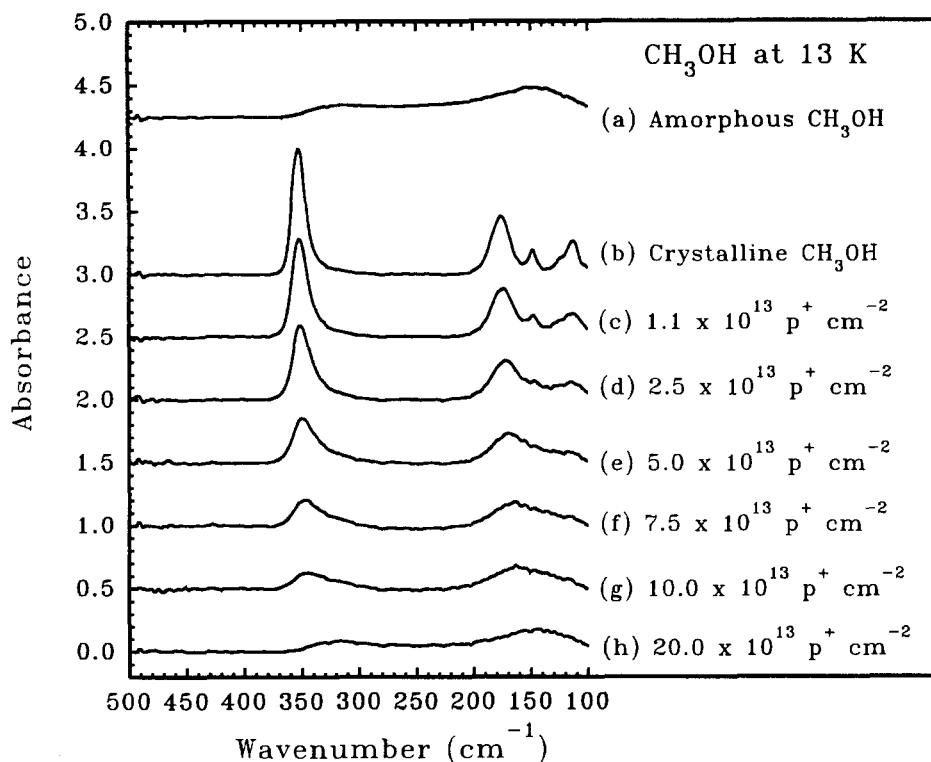


Fig. 5. Far-IR spectra of amorphous, crystalline, and irradiated  $\text{CH}_3\text{OH}$  at 13 K. Spectra have been offset vertically for clarity. The crystalline sample in (b) was obtained by warming the sample in (a) to 130 K and then recooling to 13 K. Spectra after successive 13 K irradiations are shown along with the accumulated incident fluence.

experiments. At intervals of about  $1.1 \text{ eV molecule}^{-1}$  ( $8.6 \times 10^{13} \text{ p}^+ \text{ cm}^{-2}$ ) the irradiated  $\text{H}_2\text{O}$  would release a burst of  $\text{H}_2$  as detected by a quadrupole mass spectrometer. Examination of the spectrum immediately thereafter inevitably showed that the sample had recrystallized. Further irradiation would again amorphize the sample but another  $\text{H}_2$  burst and crystallization would occur after an additional dose of about  $1.1 \text{ eV molecule}^{-1}$ . This oscillatory behavior was seen only in  $\text{H}_2\text{O}$  samples at the lowest temperatures available. It has been interpreted in terms of the build-up and sudden reaction of hydrogen atoms and is treated in a separate paper (Hudson and Moore, 1992).

Far-IR spectra of amorphous and crystalline  $\text{CH}_3\text{OH}$  at 13 K are shown in (a) and (b) of Fig. 5. The other six spectra, at the bottom of Fig. 5, are for increasing radiation doses to the sample. By comparing (a), (b), and (h) it can be seen that irradiation converted the crystalline sample's spectrum into one virtually identical to that of unirradiated amorphous  $\text{CH}_3\text{OH}$ . Figure 6 shows a similar result but at 77 K. Spectrum (a) is for the original amorphous sample, deposited at 13 K and warmed to 77 K. Spectrum (b) also was recorded at 77 K, but after a brief annealing at 130 K to crystallize the sample. The other spectra again show the effect of increasing radiation dose. As with the 13 K irradiation, the spectrum of the crys-

talline sample at 77 K is converted to one almost the same as from the unirradiated amorphous  $\text{CH}_3\text{OH}$ .

The decrease in the intense IR peak for crystalline  $\text{CH}_3\text{OH}$  near  $350 \text{ cm}^{-1}$  was used to follow the rate of radiation-induced amorphization. The analysis described earlier for irradiated  $\text{H}_2\text{O}$  also was carried out for irradiated  $\text{CH}_3\text{OH}$  to compute  $f_c$ , the fraction of crystalline sample remaining after each dose. The results are plotted in Fig. 3 for 13 and 77 K experiments (triangles and solid lines).

Figure 3 shows that the rate of loss of crystallinity on irradiation differed for  $\text{H}_2\text{O}$  and  $\text{CH}_3\text{OH}$ . There were two other ways in which these compounds differed. First, irradiated  $\text{H}_2\text{O}$  samples could be rewarmed and were always found to recrystallize. This was not the case with  $\text{CH}_3\text{OH}$ . Irradiated crystalline  $\text{CH}_3\text{OH}$  samples never were observed to crystallize on warming. Another difference in the two compounds was that some  $\text{CH}_3\text{OH}$  apparently was lost on irradiation, presumably because of product formation. This is most evident in the 77 K experiment shown in Fig. 6. The spectra at the beginning and the end of the experiment are (a) and (h) in the figure. Although the shapes are essentially the same, the bottom spectrum, corresponding to the end of the irradiations, is slightly weaker than the top one, indicating conversion of the  $\text{CH}_3\text{OH}$  sample into molecular products which did not possess strong

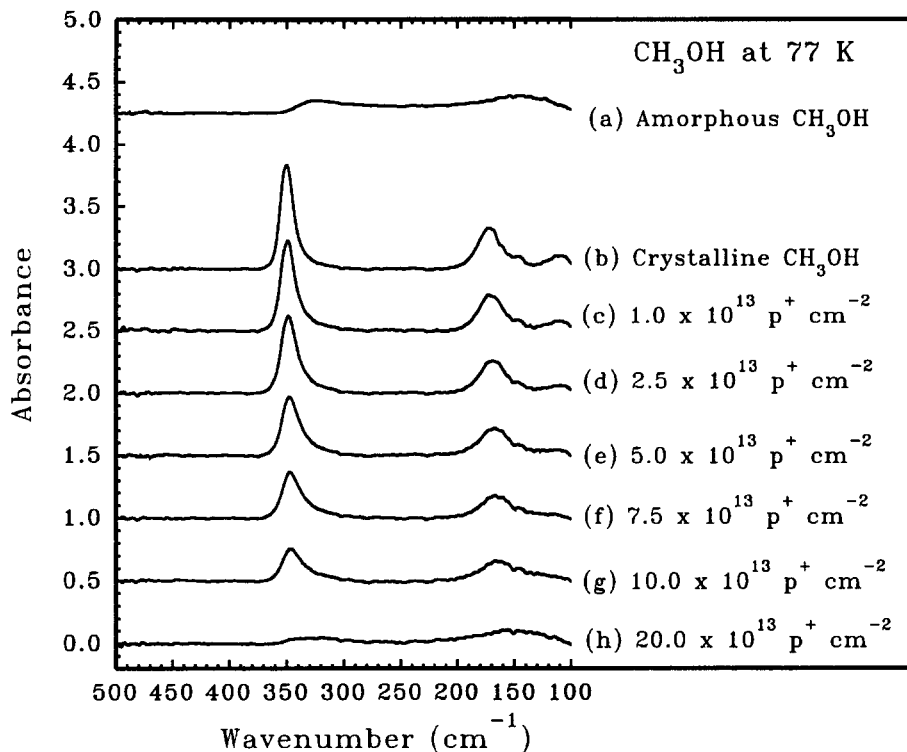


Fig. 6. Far-IR spectra of amorphous, crystalline, and irradiated  $\text{CH}_3\text{OH}$  at 77 K. Spectra have been offset vertically for clarity. The crystalline sample in (b) was obtained by warming the sample in (a) to 130 K and then recooling to 13 K. Spectra after successive 77 K irradiations are shown along with the accumulated incident fluence.

far-IR absorbances. Product formation during low-temperature radiolysis of  $\text{CH}_3\text{OH}$  has been verified by separate mid-IR studies in this laboratory. In contrast, no substantial conversion of sample to reaction products was detected in low-temperature  $\text{H}_2\text{O}$  radiation experiments (Moore and Hudson, in preparation).

Only a few irradiations were carried out on crystalline samples of  $\text{H}_2\text{CO}$  and  $\text{CO}_2$ , and all were at 13 K. Although these experiments were useful for showing loss of crystalline material, they were not pursued to the degree of those with  $\text{H}_2\text{O}$  and  $\text{CH}_3\text{OH}$ .

Formaldehyde vapor was produced for our experiments by the thermal decomposition of polyoxymethylene. Slow condensation of the  $\text{H}_2\text{CO}$  vapor at 13 K produced an amorphous  $\text{H}_2\text{CO}$  solid and its spectrum is shown as (a) in Fig. 7. Spectrum (b) in Fig. 7 is for crystalline  $\text{H}_2\text{CO}$  at 13 K, formed by warming the amorphous sample briefly from 13 to 85 K, and then recooling. Spectra (c) and (d) are after incident radiation doses of  $1 \times 10^{13}$  and  $5 \times 10^{13} \text{ p}^+ \text{ cm}^{-2}$  to the crystalline sample. The spectrum in (d) underwent only slight changes on warming the sample to room temperature. Moreover, the production of spectrum (d) on irradiation was accompanied by a visual change in the sample from transparent to white. Since the original for-

maldehyde polymer was white, and since it has essentially the same far-IR spectrum as (d) (Tadakoro *et al.*, 1963), our conclusion is that proton irradiation at 13 K caused  $\text{H}_2\text{CO}$  polymerization in the solid state.

Carbon dioxide was the fourth molecule investigated. Spectra (a) and (b) in Fig. 8 are for amorphous and crystalline  $\text{CO}_2$  at 13 K. Spectra (c) and (d) are after incident doses of  $4 \times 10^{13}$  and  $6 \times 10^{13} \text{ p}^+ \text{ cm}^{-2}$ . These spectra show that irradiation of the crystalline  $\text{CO}_2$  resulted in peak broadening and a decrease in the peak absorbance. The peak position showed a shift to smaller wavenumbers with increasing irradiation, moving away from the positions observed for crystalline and amorphous  $\text{CO}_2$ . Warming the irradiated  $\text{CO}_2$  sample sharpened the absorbance and caused it to move back toward its original position, and by 70 K the absorbance was essentially the same in shape and position as for an unirradiated  $\text{CO}_2$  sample. However, the intensity of the line after irradiation and warming was about 40% less than it would have been for an unirradiated sample at the same temperature, indicating loss of material during irradiation.

Irradiations were not carried out at 77 K for either  $\text{H}_2\text{CO}$  or  $\text{CO}_2$ . Interpretation of results at 77 K would have been complicated by a tendency of any

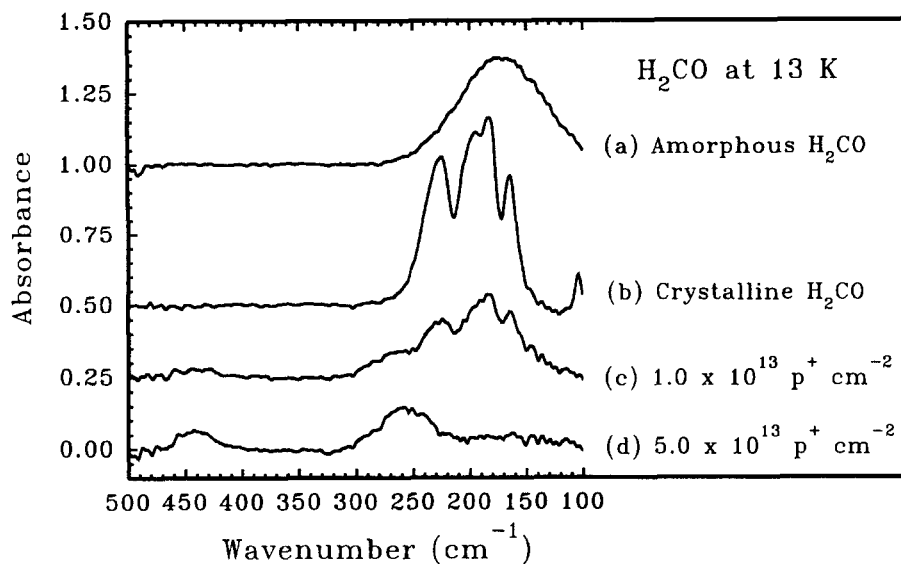


Fig. 7. Far-IR spectra of amorphous, crystalline, and irradiated formaldehyde at 13 K. Spectra have been offset vertically for clarity. The crystalline sample in (b) was obtained by warming the sample in (a) to 85 K and then recoiling to 13 K. Spectra after successive 13 K irradiations are shown along with the accumulated incident fluence.

amorphized product to recrystallize at that temperature. (This was not the case with either  $\text{H}_2\text{O}$  or  $\text{CH}_3\text{OH}$  due to the much higher temperatures needed for their crystallization.) There was also the problem that irradiation of neither crystalline  $\text{H}_2\text{CO}$  nor  $\text{CO}_2$  gave simple amorphization of the sample: the spectra produced were different from those of the unirradiated amorphous materials as shown in Figs 7 and 8.

#### DISCUSSION

Figure 3 summarizes the more quantitative aspects of our work with  $\text{H}_2\text{O}$  and  $\text{CH}_3\text{OH}$ . Using the conversions given in the experimental section allows the incident fluence to be converted into absorbed dose in units of Mrad and MGy. However, the trends of Fig. 3 are unchanged since the stopping powers of the two compounds differ only slightly, and so a revised figure is not shown. The conclusion is that at

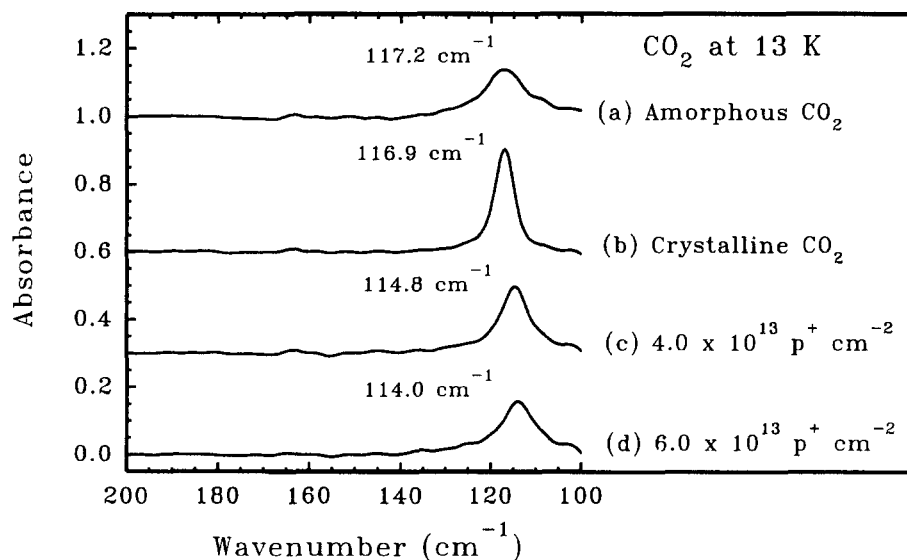


Fig. 8. Far-IR spectra of amorphous, crystalline, and irradiated carbon dioxide at 13 K. Spectra have been offset vertically for clarity. Peak positions are given in the figure to the left of the relevant absorbance band. The crystalline sample in (b) was obtained by warming the sample in (a) to 65 K and then recoiling to 13 K. Spectra after successive 13 K irradiations are shown along with the accumulated incident fluence.

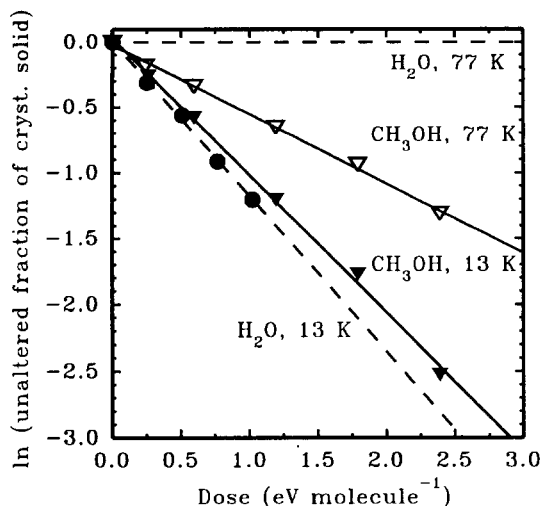


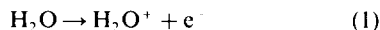
Fig. 9. Radiation-induced amorphization of  $\text{H}_2\text{O}$  and  $\text{CH}_3\text{OH}$  samples at 13 and 77 K. The units of the abscissa take into account the different stopping powers and molecular weights of the two compounds. See text for details.

both 13 and 77 K, crystalline  $\text{CH}_3\text{OH}$  is more rapidly altered by radiation than is crystalline  $\text{H}_2\text{O}$ .

While Mrad and MGy units are widely used by radiation physicists and chemists, the  $\text{eV molecule}^{-1}$  unit is more common in the astronomical community. Revising Fig. 3 with the appropriate conversions gives Fig. 9. This last figure shows that even on a per molecule basis,  $\text{CH}_3\text{OH}$  is still more radiation sensitive at 77 K than is crystalline  $\text{H}_2\text{O}$ . However at 13 K the order is reversed from Fig. 3, although admittedly the difference in the two at 13 K is slight. The reversal in going from Figs 3 to 9 simply reflects the fact that equal masses of the two compounds means fewer  $\text{CH}_3\text{OH}$  molecules than  $\text{H}_2\text{O}$  molecules, due to the different molecular masses.

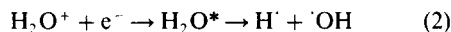
Although the experiments presented in this paper were not designed to probe details of radiation chemical mechanisms, or product yields, some consideration of reaction mechanisms seems appropriate to interpret the observations. In the past, different reaction sequences have sometimes been needed to explain experimental results from the irradiation of amorphous and crystalline materials (e.g. Kevan, 1969; Toriyama and Iwasaki, 1979). Since our experiments involve *both* types of solids, the situation is quite complicated. It is specifically not our intention to propose new mechanisms but rather to utilize those that have been reported. We consider reactions only for our  $\text{H}_2\text{O}$  and  $\text{CH}_3\text{OH}$  experiments.

The first step in the irradiation of our polycrystalline  $\text{H}_2\text{O}$  samples is



Other authors have pointed out the importance of the recombination of the two products in reaction (1) at low temperatures in solid  $\text{H}_2\text{O}$  (e.g. Seddon *et al.*,

1968; Symons, 1982). Geminate recombination leads back to  $\text{H}_2\text{O}$  and to possible dissociation.



Alternatively,  $\text{H}^+$  transfer, or equivalently H transfer, may occur after (1) so that the second and third steps will be



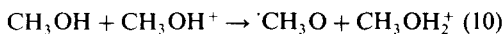
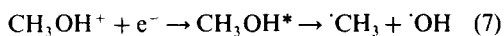
Regardless of whether (2) or (2a) + (2b) occurs, the free radicals that form are  $\text{H}^+$  and  $\cdot\text{OH}$ . Since the stopping power of 0.7 MeV protons for our samples is much greater, on the order of two orders of magnitude, than in X-ray,  $\gamma$  ray, or  $\sim 1$  MeV  $e^-$  experiments (Swallow, 1973), radical-radical reactions will be enhanced, dropping radical yields and raising molecular yields. Possible reactions are



Beyond considerations of stopping power there is irradiation temperature. The dependence of reactions (3)–(5) on temperature in irradiated  $\text{H}_2\text{O}$  ice has been studied by others (Siegel *et al.*, 1960, 1961; Flournoy *et al.*, 1962). The result is that reaction (3),  $\text{H}_2$  formation, occurs to a much greater extent than (4) and (5) for  $T < \sim 77$  K. In our experiments, any  $\text{H}_2$  produced will be retained in the solid  $\text{H}_2\text{O}$  sample much more efficiently at 13 K than at the higher temperatures (Laufer *et al.*, 1987; Kouchi and Kuroda, 1990). The higher the irradiation temperature, the more  $\text{H}_2$  is formed by reaction (3) but above about 20 K it is lost from the sample by sublimation at the ice-vacuum interface. This sublimation makes the ice appear to retain its crystallinity longer at 77 K than at 13 K, which in turn causes a variation in the constant  $k$  with temperature. At 13 K,  $\text{H}^+$  and  $\text{H}_2$  are retained in the sample during the irradiation, but lost on subsequent warming. The irradiated ice thus recrystallizes at 155 K to give the same far-IR spectrum as unirradiated crystalline ice.

Turning to our results for  $\text{CH}_3\text{OH}$ , a new set of problems is encountered since more reactions and products are possible for  $\text{CH}_3\text{OH}$  than for  $\text{H}_2\text{O}$ . Electron spin resonance has been used to study both glassy and crystalline samples of  $\text{CH}_3\text{OH}$  X-irradiated at 4.2 and 77 K (Toriyama and Iwasaki, 1979). At 4.2 K, irradiation of crystalline  $\text{CH}_3\text{OH}$  produces  $\cdot\text{CH}_3\text{O}$ ,  $\cdot\text{CH}_3$ , and  $\cdot\text{CH}_2\text{OH}$  radicals with indirect evidence for hydrogen atoms. Warming to 77 K causes loss of all  $\cdot\text{CH}_3\text{O}$  and  $\cdot\text{CH}_3$  radicals and production of more  $\cdot\text{CH}_2\text{OH}$ . Reactions, roughly analogous to (1)–(2b) for  $\text{H}_2\text{O}$ , have been proposed for the 4.2 K experiment with crystalline  $\text{CH}_3\text{OH}$ , and among these are the following:





Irradiation at 77 K gave only  $\cdot\text{CH}_2\text{OH}$  radicals as did warming 4.2 K irradiated samples to 77 K (Toriyama and Iwasaki, 1979). Glassy samples irradiated at 4.2 K gave primarily trapped electrons and  $\cdot\text{CH}_2\text{OH}$ , which in turn gave rise to other reactions.

While reactions (6)–(11) may also occur in our  $\text{CH}_3\text{OH}$  experiments, their relative importance remains unknown. Electron trapping probably increases as our sample's crystallinity drops, particularly at 13 K, so that reactions (7) and (11) will decline in importance. What is certainly expected is that radical–radical combination probably occurs to a greater degree than in experiments with radiation of lower stopping power. This will enhance the formation of molecular products such as  $\text{H}_2$  and ethylene glycol,  $(\text{CH}_2\text{OH})_2$ . By analogy with  $\text{H}_2\text{O}$  (Laufer *et al.*, 1987; Kouchi and Kuroda, 1990), we suspect that  $\text{H}_2$  is more readily held in solid  $\text{CH}_3\text{OH}$  during 13 K irradiations than in 77 K irradiations.

The greater number of radiation products from  $\text{CH}_3\text{OH}$ , as compared with the products of  $\text{H}_2\text{O}$ , are probably responsible for these compounds' different rates of amorphization. This also probably explains our inability to recrystallize irradiated  $\text{CH}_3\text{OH}$ : reaction products interfered with and prevented the crystallization. For the case of  $\text{H}_2\text{O}$ , the possible radiation reactions are more limited, and the products more easily sublimed, so that irradiated  $\text{H}_2\text{O}$  samples recrystallized on warming. Some support for the different amounts of low-temperature radiation products is provided by separate mid-IR experiments in this laboratory (Moore and Hudson, in preparation). These have verified that substantial amounts of molecular products, such as  $\text{CO}$  and  $\text{CH}_4$ , are indeed formed during low temperature proton irradiation of  $\text{CH}_3\text{OH}$ . No radiation products are detected from  $\text{H}_2\text{O}$ , although admittedly  $\text{H}_2$ ,  $\text{O}_2$ , and  $\text{H}_2\text{O}_2$  are difficult to detect with far-IR spectroscopy in solid  $\text{H}_2\text{O}$ .

The outcome of our formaldehyde radiation experiment was fundamentally different from irradiations of the other three molecules since the sample polymerized. No gradual change from the spectrum of crystalline  $\text{H}_2\text{CO}$  to that of amorphous  $\text{H}_2\text{CO}$  was observed. Low temperature  $\text{H}_2\text{CO}$  polymerization is consistent with previous radiation studies (Goldanski, 1976) including mid-IR work in this laboratory (Moore and Hudson, 1993; Moore and Tanabe, 1990).

Our  $\text{CO}_2$  irradiations showed that the far-IR spectrum of crystalline  $\text{CO}_2$  was changed on irradiation at 13 K to a spectrum that was not

matched by either pure amorphous  $\text{CO}_2$  or a combination of amorphous and crystalline  $\text{CO}_2$ . This implies that some radiation product was formed, altering the  $\text{CO}_2$  spectrum. Further evidence of this came from warming the irradiated sample: a net loss of spectral intensity was found due to the irradiation, which again implies formation of some product.  $\text{CO}$  is known to be produced by proton irradiation of solid  $\text{CO}_2$  (Moore and Hudson, in preparation), although  $\text{O}_2$  and  $\text{C}_3\text{O}_2$  are possibilities as well. An unirradiated mixture of  $\text{CO}_2$ ,  $\text{CO}$ ,  $\text{O}_2$ , and  $\text{C}_3\text{O}_2$  might conceivably be found whose spectrum would match the one we obtained for irradiated crystalline  $\text{CO}_2$ . Additional work is clearly needed.

To summarize, with each of the four compounds studied, proton irradiation resulted in loss of crystallinity. However crystalline  $\text{H}_2\text{O}$  and  $\text{CH}_3\text{OH}$  behaved differently than crystalline  $\text{H}_2\text{CO}$  and  $\text{CO}_2$ . Although the first two were largely converted into amorphous forms the latter two were not. That formaldehyde polymerized was shown by the sample's change in visual appearance and the change in IR absorbances. The fate of crystalline  $\text{CO}_2$  was not as clear, although the results imply that irradiation produced some material(s) at the expense of  $\text{CO}_2$ . It is difficult to believe that substantial amounts of any molecular products other than  $\text{CO}_2$ ,  $\text{CO}$ ,  $\text{O}_2$ , and possibly  $\text{C}_3\text{O}_2$  were present in the final irradiated sample.

Before turning to applications, some comments on low-temperature irradiations in other laboratories will be made. The experiments closest to ours have been those on  $\text{H}_2\text{O}$  in Strazzulla's laboratory. In those experiments, crystalline  $\text{H}_2\text{O}$  was irradiated at temperatures from 10 to 100 K (Strazzulla *et al.*, 1992) by 3 keV  $\text{He}^+$ . Although a quantitative comparison is difficult, the results are in qualitative agreement with our own, showing that crystalline  $\text{H}_2\text{O}$  is more resistant to radiation damage at the higher temperatures. Other experiments have used mass spectral techniques to determine identities and yields of molecules ejected during irradiation (Johnson, 1990). The measured yields are far below those needed to show changes in the remaining  $\text{H}_2\text{O}$  solid with our IR technique so again comparison is difficult. Moreover, the mass spectral measurements are made for irradiations of amorphous  $\text{H}_2\text{O}$  ice whereas the present paper is concerned primarily with irradiation of crystalline materials.

#### APPLICATIONS

There is a vast literature concerning small-molecule solids and astronomical bodies. The radiation environments of systems as diverse as cometary ices, interstellar and circumstellar ice grains, and planetary rings and satellites have all been investigated since the irradiation of such objects will influence both their properties and the appearance of their spectra (e.g. Pirronello, 1991). For example, according to our

experiments a heavily irradiated object dominated by H<sub>2</sub>O ice at  $T < \sim 77$  K will give a spectrum characteristic of an amorphous material. Such an object will have a lower thermal conductivity than a polycrystalline one (Kittel, 1949), which in turn influences the depth to which a thermal wave may penetrate. A lower thermal conductivity will affect the sublimation of volatile materials from the object, and thus the object's composition.

Comets are one example of a class of such objects. Comets are thought to have been formed at the same time as our solar system,  $4.6 \times 10^9$  years ago, and to have remained near 10 K in a roughly spherical region about a light year around our sun. Refractory grains and "frozen volatiles" such as H<sub>2</sub>O, CH<sub>3</sub>OH, H<sub>2</sub>CO, CO<sub>2</sub>, CH<sub>4</sub>, and CO compose cometary nuclei with H<sub>2</sub>O being the dominant molecule. The ices making up these nuclei are thought to be amorphous, due to their slow formation at low temperatures, although there is no direct observational evidence for their amorphous nature.

Regardless of the original phase of cometary ices, our radiation experiments suggest a different argument for the amorphous nature of the outer ices of comets, an argument based on radiation damage. The cosmic radiation dose received by a cometary nucleus about a light year from the sun will vary from  $\sim 600$  eV molecule<sup>-1</sup> at a depth of 0.1 m down to under 5 eV molecule<sup>-1</sup> at a depth near 5 m (Strazzulla and Johnson, 1991). Our experiments indicate that such doses are more than enough to cause crystalline-to-amorphous transitions. Thus comets making their initial passage about the sun will have their outer layers composed of amorphous ice, and this will influence the observed behavior of these objects.

Some years ago the crystallization of amorphous H<sub>2</sub>O was proposed to account for outbursts in comets passing the sun for the first time, so-called new comets (Patashnick *et al.*, 1974). The central assumption was that the ice on a cometary surface would be amorphous and would crystallize violently as the comet approached the sun and warmed up. However, as argued in the previous paragraph, a comet's outer layers will be exposed to and amorphized by ionizing radiation. Thus an unstated assumption is that irradiated H<sub>2</sub>O ice will crystallize on warming. At the time this picture of cometary activity was proposed there were virtually no experimental data available on the crystallization of irradiated H<sub>2</sub>O ice. The experiments presented in the present paper provide experimental support for this view of cometary outbursts. Our laboratory work demonstrates that H<sub>2</sub>O ice can indeed undergo crystallization after irradiation.

Our results can also be used to obtain information concerning the age of astronomical bodies based on a known rate of radiation-induced change at different temperatures. We can deduce the upper age limit for cosmic ices from their observed far-IR spectra by comparisons with laboratory spectra such as those in

Fig. 2. This has been done in a separate publication (Moore and Hudson, 1992) for H<sub>2</sub>O ice observed in a circumstellar envelope around the giant star designated IRAS 09371 + 1212 (Omont *et al.*, 1990). The result was an upper limit of  $10^6$  years for the object.

Even the few experiments we have performed with H<sub>2</sub>CO and CO<sub>2</sub> have astrochemical applications. Since the irradiation of H<sub>2</sub>CO causes polymerization at 13 K, astronomical observation of a solid-phase H<sub>2</sub>CO spectrum can be used to place limits on radiation exposure, although the reverse may not be true for observations of formaldehyde polymer (Schutte *et al.*, 1993). With CO<sub>2</sub>, our irradiated sample had a different spectrum than did the unirradiated sample at 13 K (Fig. 8). Thus an observation of CO<sub>2</sub> in the far-IR should reflect the radiation history of the source.

*Acknowledgements*—We thank B. Donn for many helpful discussions related to our experiments. We acknowledge D. M. Hudgins, S. A. Sandford, A. G. G. M. Tielens, and L. J. Allamandola at NASA/Ames Research Center who made optical constants available prior to publication. We thank Steve Brown and members of the GSFC/Radiation Facility for operation of the accelerator. RLH acknowledges the Administration of Eckerd College for a leave during which this work was done under an Intergovernmental Personnel Act Agreement at the NASA/Goddard Space Flight Center. Both authors acknowledge NASA funding support through grant NSG 5172. RLH also acknowledges support through NASA grant NAG-5-1843.

#### REFERENCES

- Ahmad S. R., Bridges B. J. and Charlesby A. (1980) *Radiat. Phys. Chem.* **16**, 469.  
 Becquerel H. (1901) *Comptes Rendus* **133**, 709.  
 Berman R., Klemens P. G., Simon F. E. and Fry T. M. (1950) *Nature* **166**, 866.  
 Bibring J. P., Duraud J. P., Durrieu L., Jouret C., Maurette M. and Meunier R. (1972) *Science* **173**, 753.  
 Charlesby A. (1987) Radiation chemistry of polymers. In *Radiation Chemistry* (Edited by Farhataziz and Rodgers M. A. J.), Ch. 15, and references therein. VCH Publishers, New York.  
 Fano U. (1963) *Ann. Rev. Nucl. Sci.* **13**, 1.  
 Flournoy J. M., Baum L. H. and Siegel S. (1962) *J. Chem. Phys.* **36**, 2229.  
 Goldanski V. I. (1976) *Ann. Rev. Phys. Chem.* **27**, 85.  
 Hobbs P. V. (1974) *Ice Physics*. Clarendon Press, Oxford.  
 Hudgins D. M., Sandford S. A., Allamandola L. J. and Tielens A. G. G. M. (1993) *Astrophys. J. Suppl. Ser.* **86**, 713.  
 Hudson R. L. and Donn B. (1991) *Icarus* **94**, 326.  
 Hudson R. L. and Moore M. H. (1992) *J. Phys. Chem.* **96**, 6500.  
 Johnson R. E. (1990) *Energetic Charged-Particle Interactions with Atmosphere and Surfaces*, graph p. 119 (yields). Springer, Berlin.  
 Kevan L. (1969) *Actions Chim. Biol. Radiat.* **13**, 57.  
 Kittel C. (1949) *Phys. Rev.* **75**, 972.  
 Kouchi A. and Kuroda T. (1990) *Nature* **344**, 134.  
 Laufer D., Kochavi E. and Bar-Nun A. (1987) *Phys. Rev. B* **36**, 9219.  
 Magee J. L. and Chatterjee A. (1987) Theoretical aspects of radiation chemistry. *Radiation Chemistry* (Edited by Farhataziz and Rodgers M. A. J.) Ch. 5 and references therein. VCH Publishers, New York.

- Meyer P., Ramaty R. and Webber W. (1974) *Phys. Today* **27**, 23.
- Moore M. (1984) *Icarus* **59**, 114.
- Moore M. H. and Hudson R. L. (1992) *Astrophys. J.* **401**, 353.
- Moore M. H. and Hudson R. L. Unpublished mid-IR studies of irradiated H<sub>2</sub>O, CH<sub>3</sub>OH, H<sub>2</sub>CO, and CO<sub>2</sub>; manuscript in preparation. For CH<sub>3</sub>OH see also Moore M. H., Khanna R. and Donn B. (1991). *J. Geophys. Res.* **96**, 17,541.
- Moore M. H. and Hudson R. L. (1994) *Astron. Astrophys. Suppl. Ser.* **103**, 45.
- Moore M. H. and Tanabe T. (1990) *Astrophys. J.* **365**, L139.
- Moore M., Donn B. and Hudson R. L. (1988) *Icarus* **74**, 399.
- Moore M., Donn B., Khanna R. and A'Hearn M. F. (1983) *Icarus* **55**, 388.
- Musket R. G., Hawley-Fedder R. A. and Bell W. L. (1991) *Radiat. Eff. Def. Sol.* **118**, 225.
- Narten A. H., Venkatesh C. G. and Rice S. A. (1976). *J. Chem. Phys.* **64**, 1106.
- Northcliffe L. C. and Shilling R. F. (1970) *Nucl. Data Tables A7*, 233.
- Omont A., Moseley S. H., Forveille T., Glaccum W. J., Harvey P. M., Likkell L., Loewenstein R. F. and Lisse C. M. (1990) *Astrophys. J.* **355**, L27.
- Patashnick H., Rupprecht G. and Schuerman D. (1974) *Nature* **250**, 313.
- Pirronello V. (1991) Physical and chemical effects induced by fast ions in ices of astrophysical interest. In *Chemistry in Space* (Edited by Greenberg J. and Pirronello V.), p. 263. Kluwer Academic Publishers, Dordrecht.
- Schutte W. A., Allamandola L. J. and Sandford S. A. (1993) *Science* **259**, 1143.
- Seddon W. A., Smith D. R. and Bindner P. E. (1968) *Can. J. Chem.* **46**, 1747.
- Siegel S., Flournoy J. M. and Baum L. H. (1961) *J. Chem. Phys.* **34**, 1782.
- Siegel S., Baum L. H., Skolnik S. and Flournoy J. M. (1960) *J. Chem. Phys.* **32**, 1249.
- Slichter W. P. and Mandel E. R. (1958) *J. Phys. Chem.* **62**, 334.
- Strazzulla G. and Johnson R. E. (1991) Irradiation effects on comets and cometary debris. In *Comets in the Post-Halley Era, Vol. I* (Edited by Newburn R. L., Neugebauer M. and Rahe J.), p. 243. Kluwer Academic Publishers, Dordrecht.
- Strazzulla G., Baratta G. A., Leto G. and Foti G. (1992) *Europhys. Lett.* **18**, 517.
- Swallow A. J. (1973) *Radiation Chemistry*, Ch. 2. John Wiley, New York. Stopping powers for liquid H<sub>2</sub>O are under 3 MeV/cm for ~1 MeV e<sup>-</sup>'s, e<sup>-</sup>'s from 100 kV X-rays, and Compton e<sup>-</sup>'s from <sup>60</sup>Co radiations. In comparison, the value for 0.7 MeV p<sup>+</sup> is 430 MeV/cm.
- Symons M. C. R. (1982) *Ultramicros.* **10**, 97.
- Tadakoro H., Kobayashi M., Kawaguchi Y., Kobayashi A. and Murahashi M. (1963) *J. Chem. Phys.* **38**, 703.
- Tauer K. J. and Lipscomb W. N. (1952) *Acta Crystallogr.* **5**, 606.
- Toriyama K. and Iwasaki M. (1979) *J. Am. Chem. Soc.* **101**, 2516.
- Warren S. G. (1986) *Appl. Opt.* **25**, 2650.
- Zhang L., Zhang W., Zhang Z., Yu L., Zhang H., Qi Y. and Chen D. (1992) *Radiat. Phys. Chem.* **40**, 501.

## APPENDIX

The calculation of the fraction,  $f_c$ , of crystalline H<sub>2</sub>O or CH<sub>3</sub>OH ice present after each stage of irradiation involved a linear scaling of absorbance values. The maximum value of the absorbance of the unirradiated crystalline sample was taken as one extreme and the absorbance value of the original unirradiated amorphous ice (same wavenumber, same temperature) was taken as the other extreme. Other methods of analyzing the data could have been used, such as the fitting of IR spectral band shapes, but were not found necessary in our work on H<sub>2</sub>O and CH<sub>3</sub>OH. With our data, the fits were sensitive to changes in crystallinity of about  $\pm 5\%$  in the "middle" region of crystallinity (i.e. away from the extreme values of either 100 or 0% crystallinity). This uncertainty was not a problem either at the beginning of the irradiation, since the initial sample was taken as 100% crystalline, or at the end of the experiment, since the change in crystallinity was linear on a log scale, as seen in Fig. 3.

As an example, Fig. 2(a) and (b) are for the same unirradiated sample of solid H<sub>2</sub>O at 13 K, but in 100% amorphous and 100% crystalline phases. Their absorbances at 230 cm<sup>-1</sup>, the maximum in Fig. 2(b), give the extreme values between which the absorbance of irradiated H<sub>2</sub>O will be found. The spectrum in Fig. 2(c) has an absorbance between the two extremes, the exact absorbance being dependent on the fraction,  $f_c$ , of crystalline H<sub>2</sub>O ice remaining after the irradiation. In other words,

$$A(230 \text{ cm}^{-1}) \text{ for the irradiated sample} = f_c A(230 \text{ cm}^{-1}) \text{ for the unirradiated crystalline ice} + (1 - f_c) A(230 \text{ cm}^{-1}) \text{ for the unirradiated amorphous ice}$$

where  $A(230 \text{ cm}^{-1})$  is the absorbance at 230 cm<sup>-1</sup>.